Steel and Composite Structures, Vol. 5, No. 5 (2005) 359-374

DOI: http://dx.doi.org/10.12989/scs.2005.5.5.359

Viscoplastic response and collapse of 316L stainless steel tubes under cyclic bending

Kao-Hua Chang†

Department of Engineering Science, National Cheng Kung University, Tainan, Taiwan, R.O.C.

Chien-Min Hsu‡

Department of Art-Craft, Tung Fang Institute of Technology, Kao Hsiung County, Taiwan, R.O.C.

Shane-Rong Sheu‡†

Department of Automation and Control Engineering, Far East College, Tainan, Taiwan, R.O.C.

Wen-Fung Pan‡‡

Department of Engineering Science, National Cheng Kung University, Tainan, Taiwan, R.O.C.

(Received July 30, 2004, Accepted March 28, 2005)

Abstract. This paper presents the experimental and theoretical results of the viscoplastic response and collapse of 316L stainless steel tubes subjected to cyclic bending. The tube bending machine and curvature-ovalization measurement apparatus, which was designed by Pan *et al.* (1998), were used for conducting the cyclic curvature-controlled experiment. Three different curvature-rates were controlled to highlight the characteristic of viscoplastic response and collapse. Next, the endochronic theory and the principle of virtual work were used to simulate the viscoplastic response of 316L stainless steel tubes under cyclic bending. In addition, a proposed theoretical formulation (Lee and Pan 2001) was used to simulate the relationship between the controlled cyclic curvature and the number of cycles to produce buckling under cyclic bending at different curvature-rates (viscoplastic collapse). It has been shown that the theoretical simulations of the response and collapse correlate well with the experimental data.

Key words: viscoplastic response; viscoplastic collapse; 316 L stainless steel tubes; cyclic bending; endochronic theory; moment; curvature; ovalization.

1. Introduction

The circular tube components, which are used in several industrial applications such as offshore pipelines, platforms in offshore deep water, tubular components in nuclear reactors, etc., are often

†Graduate Student, E-mail: kfchuang@cc.kuas.edu.tw
‡Associate Professor, Corresponding author, E-mail: bit@mail.tf.edu.tw
‡†Assistant Professor, E-mail: srsheu@cc.fec.edu.tw
‡‡Professor, E-mail: pan@phoebus.es.ncku.edu.tw

subjected to cyclic bending. It is well known that the ovalization of the tube cross-section is observed when a circular tube is subjected to bending. If the bending moment increases, the ovalization also increases. If a circular tube is subjected to cyclic bending, the ovalization increases with the number of cycles. Increase in ovalization causes a progressive reduction in the bending rigidity, which can result in buckling of the tube components. Therefore, the study of the response and collapse of circular tubes under bending is of importance in many industrial applications.

Since 1980, several metal tubes under monotonic or cyclic bending with or without external pressure have been investigated by several researchers, such as: the response and collapse of 6061-T6 aluminum alloy tubes under combined monotonic bending and external pressure tested by Kyriakides and Shaw (1982); the response of 6061-T6 aluminum alloy and 1018 steel tubes under cyclic bending tested by Shaw and Kyriakides (1985); the collapse of 6061-T6 aluminum alloy and 1018 steel tubes under cyclic bending tested by Kyriakides and Shaw (1987); the response and stability of 304 stainless steel tubes subjected to combined monotonic bending and external pressure studied by Corona and Kyriakides (1988); the response and buckling of 6061-T6 aluminum alloy and 1020 steel tubes under cyclic bending and external pressure discussed by Corona and Kyriakides (1991).

Subsequently, Pan *et al.* also investigated the response and collapse of circular tubes subjected to monotonic or cyclic bending. Pan *et al.* (1998) designed a new measurement apparatus, which can be placed at the mid-span of the circular tube specimen and is suitable for simultaneous experimental determinations of the tube curvature and ovalization of the tube cross-section. The 304 stainless steel tubes were cyclically bent in their study. Thereafter, Pan and Fan (1998) investigated the effect of prior curvature-rate in the preloading stage on the subsequent creep or relaxation behavior. The tubes used by them were the same as that used by Pan *et al.* (1998). Pan and Her (1998) investigated the response and stability of 304 stainless steel tubes subjected to cyclic bending with different curvature-rates. Hsu *et al.* (2000) investigated the elastoplastic response and stability of titanium alloy tubes subjected to cyclic bending and Lee and Pan (2001) investigated the viscoplastic response and stability of titanium alloy tubes subjected to cyclic bending. Lee *et al.* (2001) discussed the influence of the diameter-to-thickness ratio to the response and stability of 304 stainless steel tubes subjected to symmetrical cyclic bending. Pan and Lee (2002) studied the effect of the mean curvature on the response and collapse of 304 stainless steel tubes under cyclic bending. Lee and Pan (2002) studied the response and collapse of 304 stainless steel tubes under monotonic pure bending creep. Lee *et al.* (2004) experimentally and theoretically investigated the effect between diameter-to-thickness ratio and curvature-rate on the stability of 304 stainless steel tubes under cyclic bending.

So far, it has been found that a lot of metal tubes such as 6061-T6 aluminum alloy tubes, 1018 steel tubes, 1020 steel tubes, 304 stainless steel tubes and titanium alloy tubes have been experimentally and theoretically studied in the loading case of cyclic bending. However, a very important metal tube "316L stainless steel tubes" is lack of investigation. Previous experimental investigation has demonstrated that 316L stainless steel exhibits the viscoplastic behavior (Ikegami and Ni-Itsu 1983). Therefore, once the tube, which is fabricated by 316L stainless steel, is manipulated under cyclic bending at different loading-rate, the response and collapse of 316L stainless steel tubes for each loading-rate is expected to be generated differently. Based on this point of view, the following experimental and theoretical studies on the response and collapse of 316L stainless steel tubes subjected to cyclic bending at different curvature-rates are discussed in this paper.

For experimental aspect, a four-point bending machine (Pan *et al.* 1998, Pan and Her 1998) and a curvature-ovalization measurement apparatus, designed by Pan *et al.* (1998), were used to conduct the curvature-symmetric cyclic bending test on 316L stainless steel tubes. Based on the capacity of the bending machine, three curvature-rates, 0.0035, 0.035 and 0.35 $m^{-1}s^{-1}$, were used to demonstrate their effect on viscoplastic response and collapse of the material. By using the load cell mounted on the bending machine, the magnitude of moment can be measured. By using the side-inclinometers and the magnetic detector, the amounts of tube curvature and ovalization of the tube cross-section can be measured, respectively. In addition, the number of cycles to produce buckling were also recorded.

For theoretical aspect, the first-order ordinary differential constitutive equations of the endochronic theory, which was derived by Pan and Chern (1997), and the principle of virtual work were used to simulate the response of 316L stainless steel tubes under cyclic bending at different controlled curvature-rates. The response contains the relationship among bending moment, tube curvature and ovalization of the tube cross-section. Finally, the theoretical formulation, which was proposed by Lee and Pan (2001), was used to simulate the relationship between the controlled cyclic curvature and the number of cycles to produce buckling at different curvature-rates. Theoretical simulations of the viscoplastic response and collapse were compared with the experimental data. Good agreement between the experimental and theoretical results has been achieved.

2. Experiments

The cyclic bending experiments on 316L stainless steel tubes were conducted in a test facility, designed by Pan and his co-workers, consisting of a pure bending device and a curvature-ovalization measurement apparatus (COMA). The bending device was used for conducting the cyclic bending tests and the COMA was used for measuring the variation of tube curvature and the ovalization of the tube cross-section.

2.1 Bending device

A picture of the bending device is shown in Fig. 1. It is designed as a four-point bending machine, capable of applying bending and reverse bending. The device consists of two rotating sprockets resting on two support beams. Heavy chains run around the sprockets and are connected to two hydraulic cylinders and load cells forming a closed loop. Each tube is tested and fitted with solid rod extension. The contact between tube and the rollers is free to move along axial direction during bending. The load transfer to the test specimen is in the form of a couple formed by concentrated loads from two of the rollers. Once either the top or bottom cylinder is contracted, the sprockets are rotated, and pure bending of the test specimen is achieved. Reverse bending can be achieved by reversing the direction of flow in the hydraulic circuit. Detail description of the bending device can be found in reference of Pan *et al.* (1998).

2.2 Curvature-ovalization measurement apparatus (COMA)

The curvature-ovalization measurement apparatus (COMA), which was designed by Pan *et al.* (1998), is an instrument, which can be used to measure the tube curvature and ovalization of the tube cross-section. Fig. 2 shows a picture of the COMA. It is a lightweight instrument, which can be mounted close to the tube mid-span. There are three inclinometers in the COMA. Two of them are fixed on two holders, which are denoted as side-inclinometers. The holders are fixed on the circular tube before the test begins. Based on the fixed distance between the two side-inclinometers and the angle

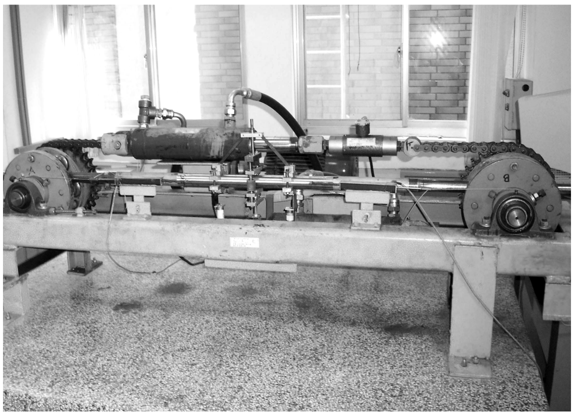

Fig. 1 A picture of the bending device

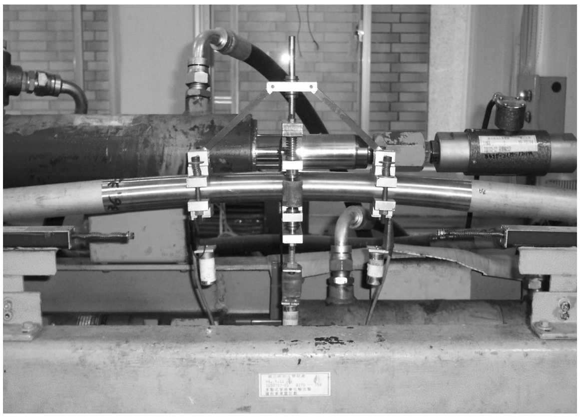

Fig. 2 A picture of the COMA

changes detected by the two side-inclinometers, the tube curvature can be obtained by simple calculation (Pan *et al.* 1998). In addition, by using the magnetic detector to measure the change of the outside diameter (middle part of the COMA), the ovalization of tube cross-section can be determined. Detailed description of the COMA can be found in the work by Pan *et al.* (1998).

2.3 Material

The material used in this study is hot-rolled 316L stainless steel tube with the chemical composition of C 0.016, Si 0.43, Mn 1.66, P 0.029, S 0.006, Cr 17.51, Ni 12.88, Mo 2.54, N 0.045 and the remainder Fe. The yield stress is 281 MPa, the ultimate tensile stress is 583 MPa and the percent elongation is 62 %. The tested specimens had a nominal outside diameter D of 36.0 mm and a wall thickness t of 0.6 mm. The D/t ratio of the tube is 60.

2.4 Experimental procedure

In this study, the cyclic bending test was conducted by using the bending machine described in

Section 2.1. The test was a curvature-controlled cyclic bending test with the curvature amplitudes varying from ± 0.15 to ± 0.45 m^{-1} and three different controlled curvature-rates of 0.0035, 0.035 and 0.35 $m^{-1}s^{-1}$. The magnitudes of the curvature and curvature-rate were controlled and measured by the COMA, which also measured the ovalization of tube cross-section. The bending moment can be calculated from the signals detected by the two load cells, mounted on the bending device. In addition, the number of cycles to produce buckling was also being recorded.

3. Problem formulation

In this section, we formulate the problem of viscoplastic response for 316L stainless steel tubes subjected to cyclic bending. The kinematics of the tube cross section, the constitutive model for viscoplastic response and the principle of virtual work are discussed separately as follows:

3.1 Kinematics

A circular tube under cyclic bending is considered in this study. Fig. 3 shows the problem geometry, in which R_m is the mean radius, and t is the wall thickness. Based on axial, circumferential, and radial coordinates x, θ and r, the displacement of a point of the tube's mid-surface are denoted as u, v and w,

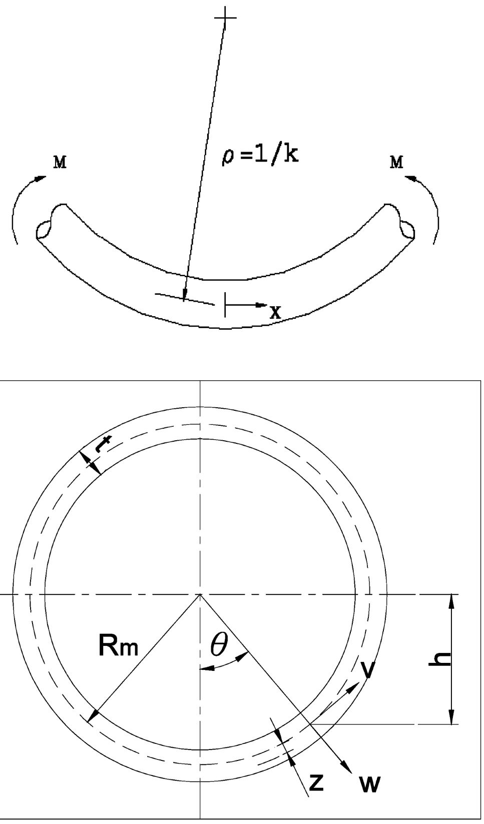

Fig. 3 Problem geometry of circular tube under pure bending

respectively. The plane sections are assumed here to be perpendicular to the tube mid-surface before and during deformation. In addition, the strains are assumed to remain small. The axial strain of the deformation is expressed as (Shaw and Kyriakides 1985, Kyriakides and Shaw 1987):

$$\varepsilon_x = \varepsilon_x^0 + h \cdot k \tag{1}$$

and

$$h = (R_m + w)\cos\theta - v\sin\theta + Z\cos\theta \tag{2}$$

where ε_x^0 is the axial strain of the cylinder's axis, h is distance between a point and horizontal plane passed through the center of the cross-section, κ is the tube curvature and Z is the distance between a point and mean surface. The circumferential strain is

$$\varepsilon_\theta = \varepsilon_\theta^0 + h\kappa_\theta \tag{3}$$

where

$$\varepsilon_\theta^0 = \frac{(v' + w)}{R_m} + \frac{1}{2}\left(\frac{v' + w}{R_m}\right)^2 + \frac{1}{2}\left(\frac{v - w'}{R_m}\right)^2 \tag{4}$$

and

$$k_\theta = \left(\frac{v' - w''}{R_m^2}\right) \Big/ \sqrt{1 - \left(\frac{v - w'}{R_m}\right)^2}\,. \tag{5}$$

(') denotes the differentiation with respect to θ.

3.2 Endochronic constitutive equations

The endochronic theory is adopted for simulating the viscoplastic response of circular tubes under cyclic bending. Owing to the highly nonproportional path of the stress history, the incremental form of endochronic theory should be considered in formulating the problem. According to the condition of small deformation for homogeneous and isotropic materials, the increment of deviatoric stress tensor $d\underset{\sim}{s}$ of endochronic theory is given as (Valanis 1980)

$$d\underset{\sim}{s} = 2\rho(0)d\underset{\sim}{e}^p + 2\underset{\sim}{h}(z)dz \tag{6}$$

and

$$\underset{\sim}{h}(z) = \int_0^z \frac{d\rho(z - z')}{dz}\frac{\partial \underset{\sim}{e}^p}{dz'} \tag{7}$$

where z is the intrinsic time scale, $\rho(z)$ is termed the kernel function and $\underset{\sim}{e}^p$ is the deviatoric plastic strain tensor which is defined as

$$d\underset{\sim}{e}^p = d\underset{\sim}{e} - \frac{d\underset{\sim}{s}}{2\mu_0} \tag{8}$$

where $\underset{\sim}{e}$ denotes the deviatoric strain tensor, μ_0 is the elastic shear modulus. The intrinsic time measure ζ is

$$d\zeta = k\|d\underset{\sim}{e}^p\| \tag{9}$$

in which $\|\cdot\|$ represents the Euclidean norm and k is the rate-sensitivity function. The function k for describing the viscoplastic behavior of material under multiaxial loading is expressed as (Pan and Chern 1997):

$$k = 1 - k_s \log\left[\frac{\dot{e}^p_{eq}}{(\dot{e}^p_{eq})_0}\right] \tag{10}$$

where k_s is a rate-sensitivity parameter, $(\dot{e}^p_{eq})_0$ is the reference equivalent deviatoric plastic strain-rate, and $\dot{e}^p_{eq}$ is the relative equivalent deviatoric plastic strain-rate. The material function (or hardening function) $f(\zeta)$ is

$$f(\zeta) = \frac{d\zeta}{dz} = 1 - Ce^{-\beta\zeta}, \quad \text{for } C < 1 \tag{11}$$

in which C and β are material parameters. If the plastic incompressibility is satisfied, the elastic hydrostatic response can be written as

$$d\sigma_{kk} = 3Kd\varepsilon_{kk} \tag{12}$$

where σ_{kk} and ε_{kk} are the trace of stress and strain tensors, respectively, and K is the elastic bulk modulus. According to the mathematical characteristic of the kernel function $\rho(z)$, Eq. (6) is expressed as (Pan and Chern 1997)

$$d\underset{\sim}{s} = \sum_{i=1}^{n} d\underset{\sim}{s}_i = 2\sum_{i=1}^{n} C_i d\underset{\sim}{e}^p - \sum_{i=1}^{n} \alpha_i \underset{\sim}{s}_i dz \tag{13}$$

where C_i and α_i are material constants. Substituting Eq. (8) into Eq. (13) leads to

$$d\underset{\sim}{s} = \frac{\mu_0}{\mu_0 + \sum_{i=1}^{n} C_i}\left[2\sum_{i=1}^{n} C_i d\underset{\sim}{e} - \sum_{i=1}^{n} \alpha_i \underset{\sim}{s}_i dz\right] \tag{14}$$

By using Eq. (12), Eq. (14) can be expressed in terms of the stress and strain tensors as

$$d\underset{\sim}{\sigma} = p_1 d\underset{\sim}{\varepsilon} + p_2 d\varepsilon_{kk}\underset{\sim}{I} + p_3 \sum_{i=1}^{n} \alpha_i \left(\underset{\sim}{\sigma} - \frac{\sigma_{kk}}{3}\underset{\sim}{I}\right)_i dz \tag{15}$$

where

$$p_1 = \frac{2\rho(0)}{1+\frac{\rho(0)}{\mu_0}}, \quad p_2 = K - \frac{2\rho(0)}{3\left(1+\frac{\rho(0)}{\mu_0}\right)}, \quad p_2 = \frac{1}{1+\frac{\rho(0)}{\mu_0}} \tag{16}$$

3.3. Principle of virtual work

The principle of virtual work, which satisfied the equilibrium requirement, is given by

$$\int_V \sigma_{ij}\delta\varepsilon_{ij}dV = \delta W \tag{17}$$

where V is the volume of the material of the tube section considered, and δW is the virtual work of the external loads. For the case of a circular tube subjected to cyclic bending, the quantity of δW is expressed for the incremental loading to be

$$\int_V (\sigma_{ij} + \dot{\sigma}_{ij})\delta\dot{\varepsilon}_{ij}dV = 2R\int_0^{\pi} \int_{-t/2}^{t/2} [\hat{\sigma}_x \delta\dot{\varepsilon}_x]dTd\theta = 0 \tag{18}$$

where $\hat{\sigma}_x = \sigma + \sigma_x$ and $(\dot{\ })$ denotes the increment of ( ). The in-plane displacement v and w are assumed to be symmetrical and are approximated by the following expression (Shaw and Kyriakides 1985, Kyriakides and Shaw 1987):

$$v \cong R_m \sum_{n=2}^{N} a_n \sin n\theta, \quad w \cong R_m \sum_{n=0}^{N} b_n \cos n\theta \tag{19}$$

where the number of terms N is chosen to ensure satisfactory convergence. Kyriakides and Shaw (1987) investigated the sensitivity of the moment-curvature and ovalization-curvature response for monotonic pure bending to the number of expansion terms used in Eq. (19). Those equations clearly indicate that $N = 4$ or 6 is sufficient. By substituting Eqs. (1)-(5), (19) into Eq. (18), a system of $2N+1$ nonlinear algebraic equations in terms of $\dot{a}_2$, $\dot{a}_3$,…., $\dot{b}_0$, $\dot{b}_1$, $\dot{b}_2$,…, $\dot{\varepsilon}_x^0$ are determined. This system of equations is solved using the Newton-Raphson method. The iterative scheme contains nested iterations for the constitutive relations. Kyriakides and Shaw (1987) provide a more detailed derivation of the system of equations.

4. Comparison and discussion

In this section, we compared the theoretical simulation of the viscoplastic response of 316L stainless steel tubes under cyclic bending with the experimental data. In the theoretical study, the kernel function of the endochronic theory was considered to be composed by three terms of exponentially decaying function, therefore, the material parameters of the theory can be determined according to the method proposed by Fan (1983). The material parameters were determined to be: $\mu_0 = 70$ GPa, $K = 150$ GPa, $C_1 = 4.3\times10^6$ MPa, $\alpha_1 = 5800$, $C_2 = 3.6\times10^5$ MPa, $\alpha_2 = 1200$, $C_3 = 2.4\times10^4$ MPa, $\alpha_3 = 450$, $C = 0.25$, $\beta = 10$, and $k_s = 0.025$. Finally, the viscoplastic collapse of 316L stainless steel tubes under cyclic bending is

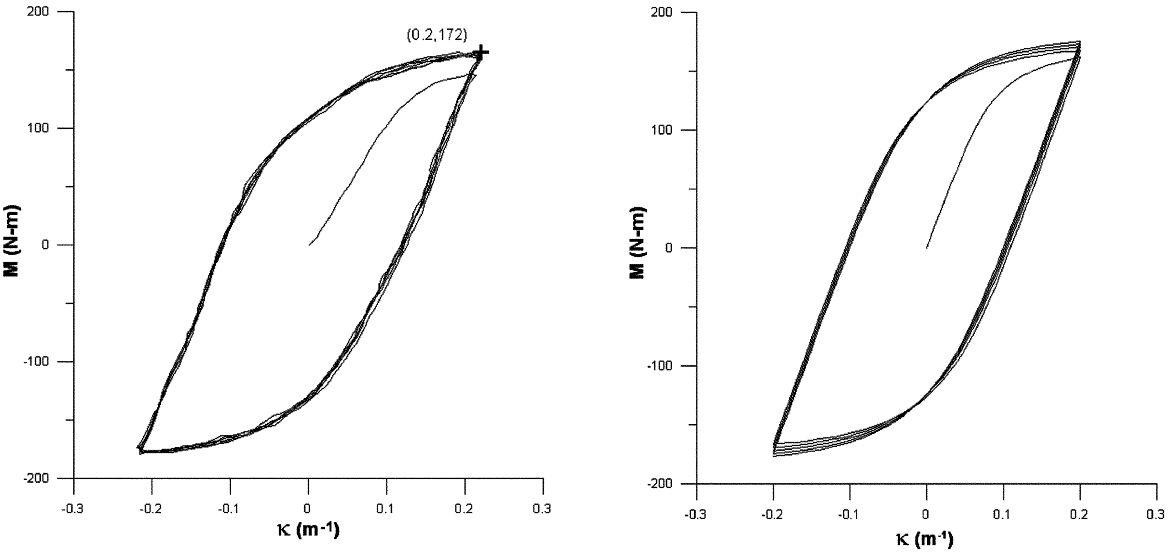

(a) Experiment (b) Theory

Fig. 4 Experimental and simulated moment (M) – curvature (κ) curves at the curvature-rate of 0.0035 $m^{-1}s^{-1}$

also discussed. Theoretical formulation, which was proposed by Lee and Pan (2001), was used to simulate the relationship between the controlled cyclic curvature and the number of cycles to produce buckling at different curvature-rates.

4.1. Viscoplastic response of 316L stainless steel tubes under cyclic bending

Figs. 4(a), 5(a) and 6(a) present typical experimental results of cyclic moment (M) - curvature (κ) curve for 316L stainless steel tube under the curvature-rates of 0.0035, 0.035 and 0.35 $m^{-1}s^{-1}$, respectively. The magnitude of the cyclic curvature range from + 0.2 m^{-1} to - 0.2 m^{-1}. It is observed from the moment-curvature curve for each controlled curvature-rate that the 316L stainless steel tube is cyclically harden and gradually steady after a few cycles for symmetric curvature-controlled cyclic bending. It can be seen that the $M-\kappa$ curves of Figs. 4(a), 5(a) and 6(a) are very similar (the magnitudes of the maximum moment at the curvature of + 0.2 m^{-1} are 172, 174 and 176 N-m, respectively) This indicates that the curvature-rate does not have too much influence on the $M-\kappa$ curve. Figs. 4(b), 5(b) and 6(b) show the corresponding simulated results obtained by the theoretical formulation described in Section 3. Figs. 7(a), 8(a) and 9(a) depict the corresponding experimental ovalization of tube cross-section as a function of the applied curvature for Figs. 4(a), 5(a) and 6(a), respectively. The ovalization is defined as $\Delta D/D$ where D is the outer diameter and ΔD is the change in outer diameter. It can be noted that for each controlled curvature-rate the ovalization of tube cross-section increases in a ratcheting manner with the number of cycles. As the cyclic process continues, the ovalization keeps accumulating. If one compares the ($\Delta D/D$)-κ curves for different controlled curvature-rates, the higher degree of the ovalization can be noticed under higher curvature-rates. This indicates that the curvature-rate have a strong influence on the ($\Delta D/D$)-κ curve. Figs. 7(b), 8(b) and 9(b) show the corresponding simulated results of ($\Delta D/D$)-κ curve.

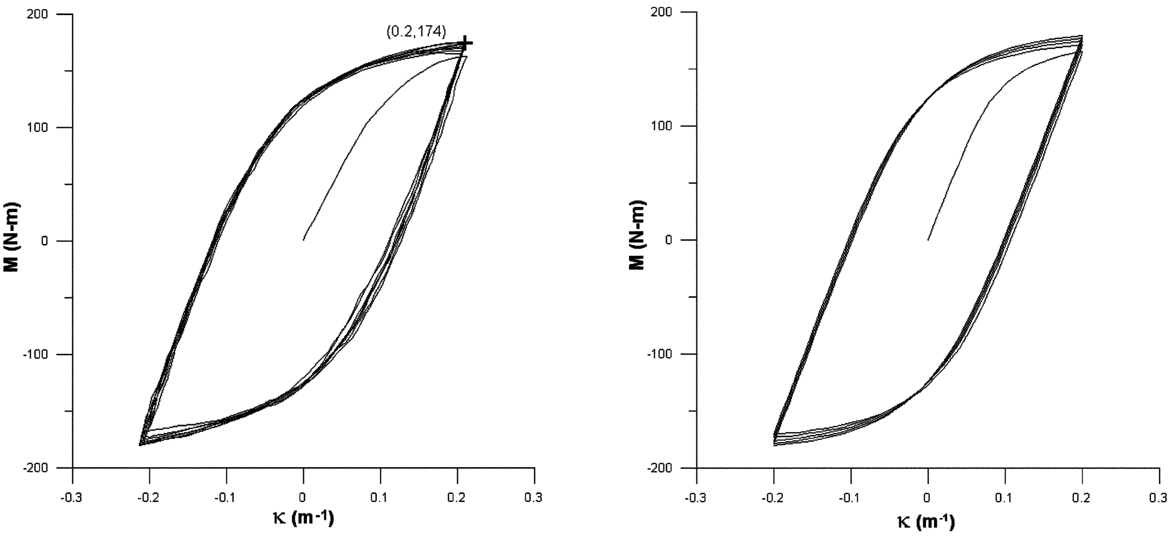

(a) Experiment (b) Theory

Fig. 5 Experimental and simulated moment (M) – curvature (κ) curves at the curvature-rate of 0.035 $m^{-1}s^{-1}$

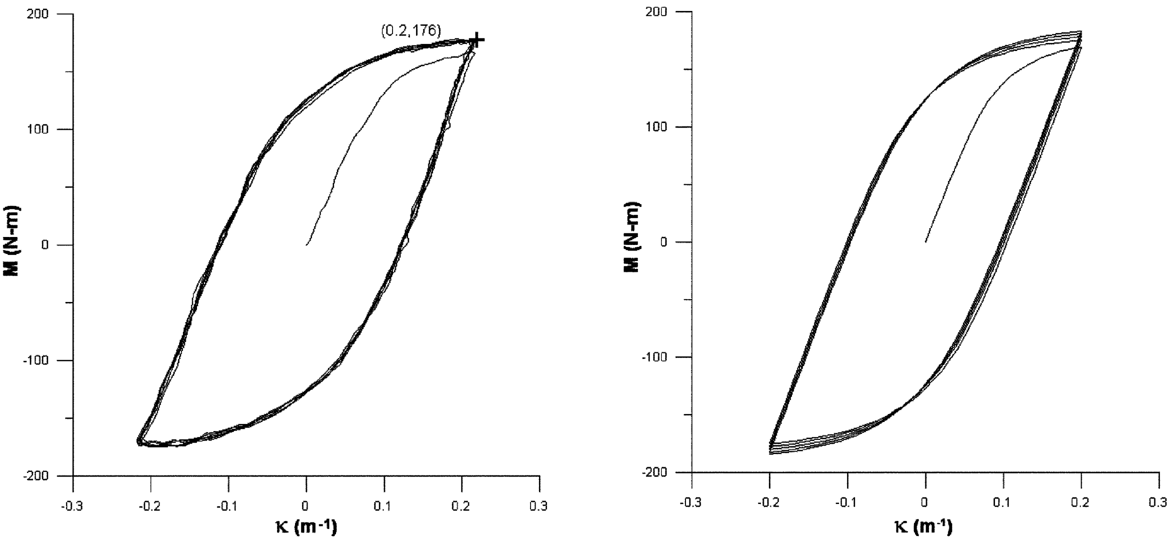

(a) Experiment (b) Theory

Fig. 6 Experimental and simulated moment (M) – curvature (κ) curves at the curvature-rate of 0.35 $m^{-1}s^{-1}$

4.2. Collapse of 316L stainless steel tubes under cyclic bending

Fig. 10 demonstrates the ovalization at buckling $(\Delta D/D)_b$ versus the magnitude of cyclic curvature (κ_c) for all tested 316L stainless steel tubes. Although the magnitudes of κ_c are different and the controlled curvature-rates are also different, the ovalizations at buckling are approximately the same

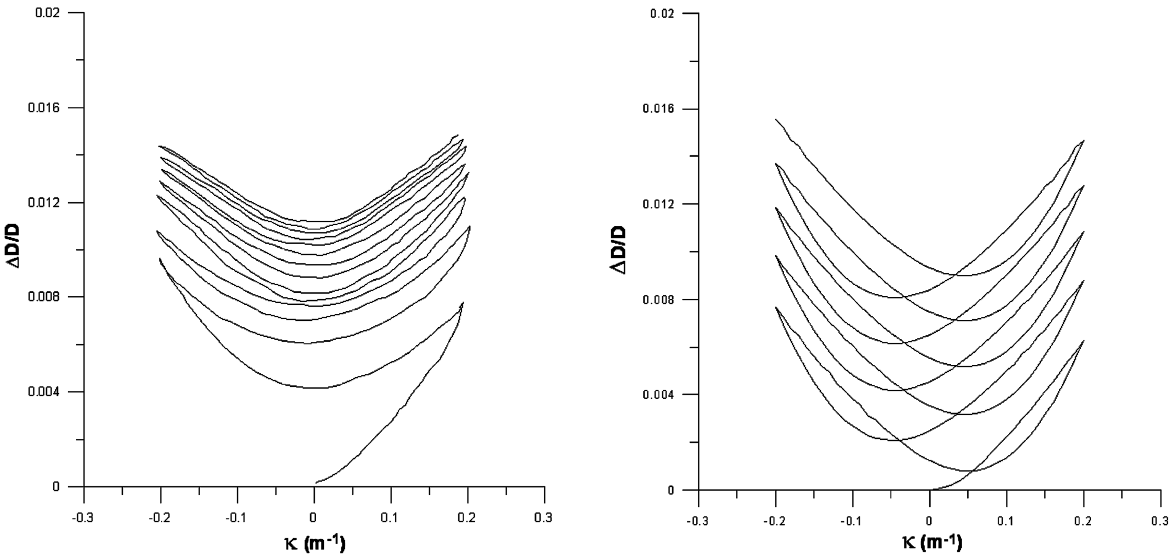

(a) Experiment (b) Theory

Fig. 7 Experimental and simulated ovalization ($\Delta D/D$)–curvature (κ) curves at the curvature-rate of 0.0035 $m^{-1}s^{-1}$

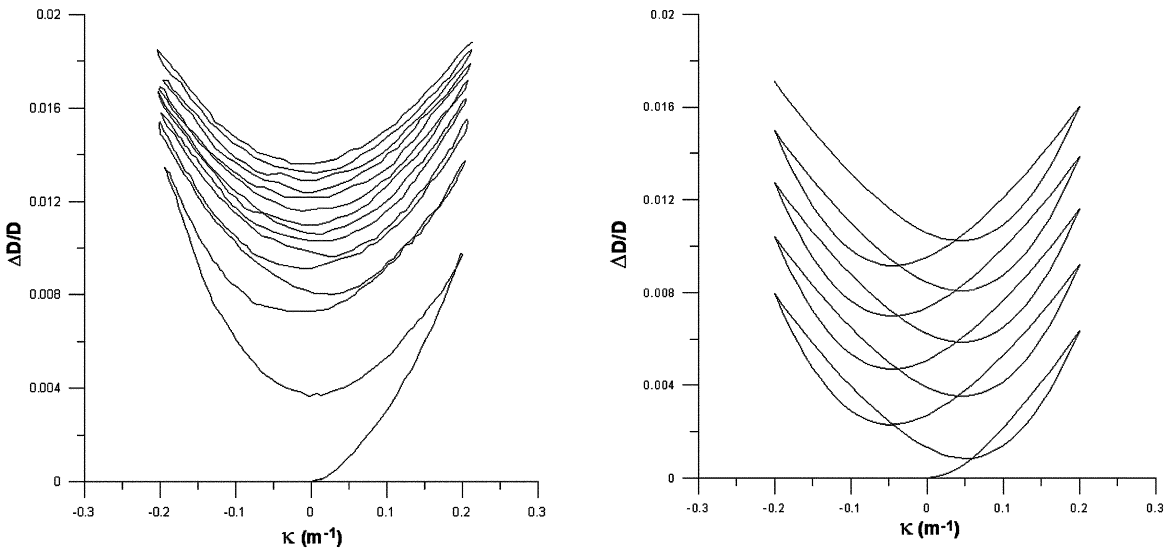

(a) Experiment (b) Theory

Fig. 8 Experimental and simulated ovalization ($\Delta D/D$) – curvature (κ) curves at the curvature-rate of 0.035 $m^{-1}s^{-1}$

($(\Delta D/D)_b \doteqdot 0.031$). A similar test result was also reported by Kyriakides and Shaw (1987) for 606l-T6 aluminum and l018 steel tubes and Hsu *et al.* (2000) for titanium alloy tubes. But their cases were considered the symmetric cyclic bending at a constant curvature-rate. Fig. 11 shows a picture of the local buckling of the 316L stainless steel tubes under cyclic bending. The magnitude of cyclic curvature (κ_c) versus the number of cycles to produce buckling (N_b) is shown in Fig. 12, wherein the magnitudes

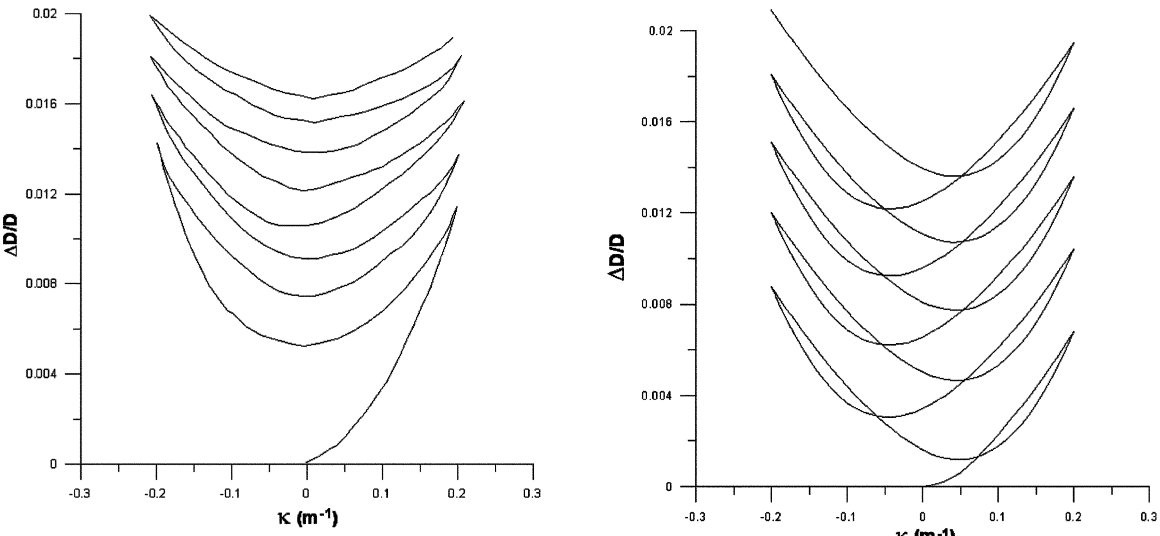

(a) Experiment

(b) Theory

Fig. 9 Experimental and simulated ovalization ($\Delta D/D$) – curvature (κ) curves at the curvature-rate of 0.35 m^{-1}s^{-1}

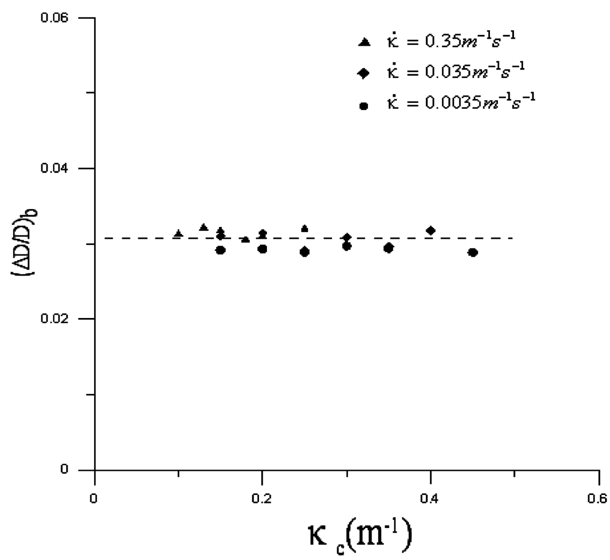

Fig. 10 Ovalization at buckling $(\Delta D/D)_b$ versus the cyclic curvature (κ_c) for all tested 316L stainless steel tubes

of cyclic curvatures were varied from ± 0.10 to ± 0.45 m^{-1} and three different controlled curvature-rates were 0.0035, 0.035 and 0.35 m^{-1}s^{-1}. The same result plotted on log-log scale is shown in Fig. 13. The experimental data of κ_c versus N_b on log-log scale almost fall on three straight lines for three different curvature-rates. The solid lines are determined by the least-square method.

Kyriakides and Shaw (1987) have proposed a formulation of the relationship between κ_c and N_b for the material tested by them as

Fig. 11 A picture of the local buckling of the 316L stainless steel tubes subjected to cyclic bending

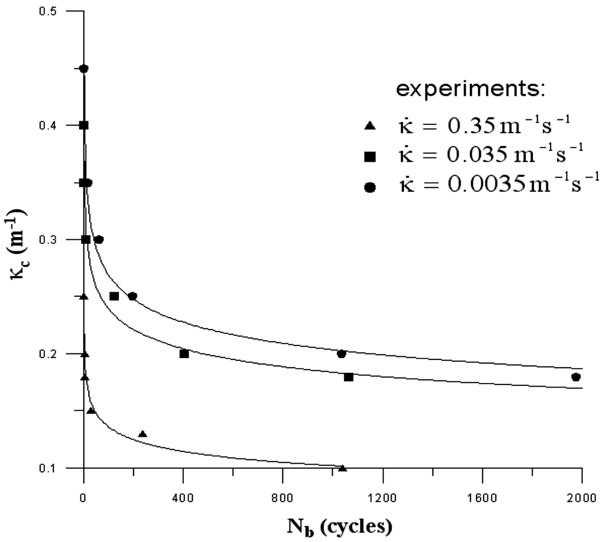

Fig. 12 Cyclic curvature (κ_c) versus the number of cycles to produce buckling (N_b) at three different curvature-rates

$$k_c = A(N_b)^{-\alpha} \quad \text{or} \quad \log\kappa_c = \log A - \alpha\log N_b \tag{20a,b}$$

where A and α are the material parameters, which are related to the material properties and the D/t ratio. The material parameter A is the controlled cyclic curvature magnitude at $N_b = 1$, and α is the slope in the log-log plot (Eq. (20b)). Based on the experimental data of circular tubes with $D = 31.75$ mm and $t = 0.889$ mm ($D/t = 35.7$), reported by Kyriakides and Shaw (1987), the magnitudes of A and α were calculated to be: $A = 0.968$ m^{-1} and $\alpha = 0.078$ for 1018 steel and $A = 0.988$ m^{-1} and $\alpha = 0.078$ or 0.12 for 6061-T6 aluminum. Based on the experimental data of titanium alloy tubes with $D = 25.4$ mm and $t = 0.7$ mm ($D/t = 36.3$), reported by Hsu *et al.* (2001), the magnitudes of A and α were calculated to be:

A=0.314 m^{-1} and α = 0.191.

As for the viscoplastic effect, Pan and Her (1998) proposed a formulation of the relationship among κ_c, N_b and the controlled curvature-rate ($\dot{\kappa}$) for 304 stainless steel tubes to be:

$$\kappa_c = B\,(N_b)^{-\alpha} \tag{21}$$

where B is a function of the curvature-rate, and was expressed as

$$B = B_o + \beta\left[\log\frac{\dot{\kappa}}{\dot{\kappa}_o}\right]^2 \tag{22}$$

where B_o is the material parameter for lowest curvature-rate and $\dot{\kappa}_o$ is the lowest curvature-rate, $\dot{\kappa}$ is the other relative curvature-rate and β is the material parameter. In 2001, Lee and Pan (2001) investigated the viscoplastic effect on the titanium alloy tubes subjected to cyclic bending. A modified formulation of Eq. (22) was proposed to be

$$B = B_o + \beta\left[\log\frac{\dot{\kappa}}{\dot{\kappa}_o}\right]^n \tag{23}$$

where n is the material parameter. For circular tubes of 304 stainless steel, the magnitude of n is equal to 2 (which was used by Pan and Her 1998). In their investigation, the magnitudes of B_o, α, β and n for titanium alloy tubes with D/t ratio of 36.3, were determined to be 1.5529 m^{-1}, 0.191, 0.1049 and 0.9504, respectively. As for 316L stainless steel tubes with D = 36.0 mm and t = 0.6 mm (D/t = 60), the material parameters B_o, α, β and n were calculated to be 0.496 m^{-1}, 0.143, 0.084 and 1.552, respectively. The dotted lines in Fig. 13 are the simulated result by using Eqs. (21) and (23). Good agreement between the theoretical and experimental results has been achieved when compared with the experimental result.

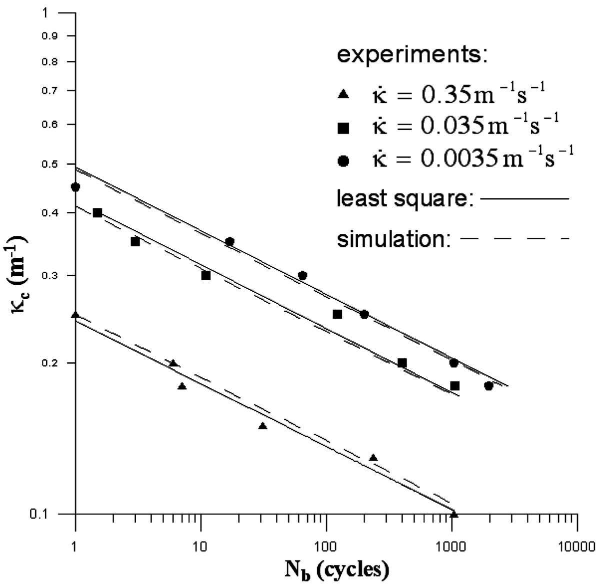

Fig. 13 Cyclic curvature (κ_c) versus the number of cycles to produce buckling (N_b) at three different curvature-rates (log-log scales)

5. Conclusions

The viscoplastic response and collapse of 316L stainless steel tubes subjected to cyclic bending are investigated experimentally and theoretically in this study. A bending machine and a curvature-ovalization measurement apparatus were used for conducting the symmetric curvature-controlled cyclic bending tests. The endochronic theory and the principle of virtual wok were used for constructing the theoretical formulation. Based on the experimental and theoretical results, the following important conclusions can be drawn:

(1) It is found from the M–κ curves that the 316L stainless steel tube is cyclically hardened and gradually steady after a few cycles under symmetric curvature-controlled cyclic bending. However, the curvature-rate has a slight influence on the $M-\kappa$ curve. It is observed from the $(\Delta D/D)$-κ curves that the ovalization of the tube cross-section increases in a ratcheting manner with the number of cycles. However, the curvature-rate has a strong influence on the $(\Delta D/D)$-κ curve.

(2) The endochronic theory and the principle of virtual work were used to investigate the response of 316L stainless steel tubes subjected to cyclic bending at different curvature-rates. It can be seen that the theoretical simulations correlate well with the experimental results.

(3) Under cyclic symmetric curvature-controlled bending, the 316L stainless steel tubes show progressive increase in the ovalization of the tube cross-section. The tubes will buckle when the ovalization accumulates to a critical value. The maximum ovalizations reached in all tested 316L stainless steel tubes at any different curvature-rate are approximately same.

(4) A formulation of the relationship among κ_c, N_b and $\dot{\kappa}$, proposed by Lee and Pan (2001), was used for constructing the same relationship for the 316L stainless steel tubes in this paper. The material constants B_o, α, β and n for 316L stainless steel tubes with D = 36.0 mm and t = 0.6 mm (D/t = 60) were calculated to be: 0.496 m^{-1}, 0.143, 0.084 and 1.552. Theoretical and experimental results are in good agreement.

Acknowledgements

The reported experimental work was carried out by using the bending facilities developed by Professor Wen-Fung Pan (Department of Engineering Science, National Cheng Kung University). His support is gratefully acknowledged.

References

Corona, E. and Kyriakides, S. (1988), "On the collapse of inelastic tubes under combined bending and pressure", *Int. J. Solids Struct.*, **24**(5), 505-535.

Corona, E. and Kyriakides, S. (1991), "An experimental investigation of the degradation and buckling of circular tubes under cyclic bending and external pressure", *Thin-Walled Struct.*, **12**, 229-263.

Fan. J. (1983), "A comprehensive numerical study and experimental verification of endochronic plasticity", Ph.D. Dissertation, Department of Aerospace Engineering and Applied Mechanics, University of Cincinnati.

Ikegami, K. and Ni-Itsu, Y. (1983), "Experimental evaluation of the interaction effect between plastic and creep deformation", *Plasticity Today Symposium*, Udine, Italy, 27-30.

Kyriakides, S. and Shaw, P.K. (1982), "Response and stability of elastoplastic circular pipes under combined

bending and external pressure", *Int. J. Solids Struct.*, **18**(11), 957-973.
Kyriakides, S. and Shaw, P.K. (1987), "Inelastic buckling of tubes under cyclic loads", ASME *J. Press. Vessel Technol.*, **109**, 169-178.
Lee, K.L. and Pan, W.F. (2001), "Viscoplastic collapse of titanium alloy tubes under cyclic bending", *Struct. Engng. Mech., An Int. J.*, **11**(3), 315-324.
Lee, K.L. and Pan, W.F. (2002), "Pure bending creep of SUS 304 stainless steel tubes", *Steel and Comp. Struct., An Int. J.*, **11**(3), 315-324.
Lee, K.L., Pan, W.F. and Kuo, J.N. (2001), "The influence of the diameter-to-thickness ratio on the stability of circular tubes under cyclic bending", *Int. J. Solids Struct.*, **38**, 2401-2413 .
Lee, K.L., Pan, W.F. and Hsu, C.M. (2004), "Experimental and theoretical evaluations of the effect between diameter-to-thickness ratio and curvature-rate on the stability of circular tubes under cyclic bending", *JSME International Journal, Series A*, **47**(2), 212-222.
Pan, W.F. and Chern, C.H. (1997), "Endochronic description for viscoplastic behavior of materials under multiaxial loading", *Int. J. Solids Struct.*, **34**(17), 2131-2159.
Pan, W.F. and Fan, C.H. (1998), "An experimental study on the effect of curvature-rate at preloading stage on subsequent creep or relaxation of thin-walled tubes under pure bending", *JSME International Journal, Series A*, **41**(4), 525-531.
Pan, W.F. and Her, Y.S. (1998), "Viscoplastic collapse of thin-walled tubes under cyclic bending", ASME *J. Engng. Mat. Tech.*, **120**, 287-290.
Pan, W.F. and Lee, K.L. (2002), "The effect of mean curvature on the response and collapse of thin-walled tubes under cyclic bending", *JSME International Journal, Series A*, **45**(2), 309-318.
Pan, W.F., Wang, T.R. and Hsu, C.M. (1998), "A curvature-ovalization measurement apparatus for circular tubes under cyclic bending", *Experimental Mechanics*, *An Int. J.*, **38**(2), 99-102.
Shaw, P.K. and Kyriakides, S. (1985), "Inelastic analysis of thin-walled tubes under cyclic bending", *Int. J. Solids Struct.*, **21**(11), 1073-1110.
Valanis, K.C. (1980), "Fundamental consequence of a new intrinsic time measure-plasticity as a limit of the endochronic theory", *Arch. Mech.*, **32**, 171-191.

CC